Periodica Polytechnica Electrical Engineering and Computer Science, 64(1), pp. 64–73, 2020

Improved Sensorless Control of Doubly Fed Induction Motor Drive Based on Full Order Extended Kalman Filter Observer

Djamila Cherifi[1*], Yahia Miloud[1]

[1] GACA Laboratory, Department of Electrical Engineering, Faculty of Technology, University of Dr. Tahar Moulay, P. O. B. 138, 20000 Ennasr, Saida, Algeria
[*] Corresponding author, e-mail: d_cherifi@yahoo.fr

Received: 20 April 2019, Accepted: 16 July 2019, Published online: 30 October 2019

Abstract

The paper deals with a Doubly Fed Induction Motor (DFIM) supplied by two PWM voltages inverters. The aims of this paper are sensorless adaptive Fuzzy-PI speed control decoupled by a vector control applied to a Doubly Fed Induction Motor using full order Extended Kalman Filter. The application of the adaptive Fuzzy-PI controller for speed control brings a very interesting solution to the problems of robustness and dynamics. In order to reduce the number of sensors used, and thus the cost of installation, Extended Kalman Filter Observer is used to estimate the rotor speed, rotor fluxes and stator currents, this observer is a unique observer which offers best possible filtering of the noise in measurement and of the system if the noise covariances are known. Simulation results of the proposed scheme show good performances.

Keywords

Doubly Fed Induction Motor (DFIM), Direct Field Oriented Control (DFOC), robust adaptive Fuzzy-PI controller, sensorless control, Extended Kalman Filter Observer (EKFO)

1 Introduction

Nowadays, the Doubly Fed Induction Motor (DFIM) drives are becoming popular in industry applications due to its high power handling capability without increasing the power rating of the converters. It presents good performances stability both in very low speed and in high speed operation [1, 2]. The progress accomplished, in the few past years, in power electronics has made the Doubly Fed Induction Motor (DFIM) an industrial standard due to its low cost and high reliability [3, 4]. DFIM is essentially non-linear, due to the coupling between the flux and the electromagnetic torque. Vector control with directed rotor flux has become the most widely used technique for variable speed electric drives of asynchronous motors. It consists in finding a situation similar to that found in the DC machine, controlling the flux and the torque independently [5-7]. However, the performance is sensitive to the variations of machine parameters, because the control laws using the PI type controllers give good results in the case of linear systems with constant parameters, but for nonlinear systems, these conventional control laws can be insufficient because they are not robust especially when the requirements on the speed and other dynamic characteristics of the system are strict. In order to improve the performance of the vector control and make it insensitive to parameter variations, and disturbances, we propose an adaptive Fuzzy-PI speed controller. Vector control based adaptive Fuzzy-PI speed controller provides precise speed control in a wide range of variation with high static and dynamic performance. The drawback of this method is that the rotor speed of the DFIM must be measured, which requires a speed sensor of some kind, for example a resolver or an incremental encoder. The cost of the speed sensor, at least for machines with ratings less than 10 kW, is in the same range as the cost of the motor itself. The mounting of the sensor to the motor is also an obstacle in many applications. A sensor less system where the speed is estimated instead of measured would essentially reduce the cost and complexity of the drive system. Note that the term sensor less refers to the absence of a speed sensor on the motor shaft, and that motor currents and voltages must still be measured. The vector control method requires also estimation of the flux linkage of the machine, whether the speed is estimated or not [8-10]. Various control algorithms have been proposed

Cite this article as: Cherifi, D., Miloud, Y. "Improved Sensorless Control of Doubly Fed Induction Motor Drive Based on Full Order Extended Kalman Filter Observer", Periodica Polytechnica Electrical Engineering and Computer Science, 64(1), pp. 64–73, 2020. https://doi.org/10.3311/PPee.14245

for the elimination of speed and position sensors: estimators using state equations, artificial intelligence, Model Reference Adaptive System (MRAS), Extended Kalman Filters (EKF), Extended Luenberger Observer (ELO), sliding mode observer ect. ... [11]. This paper proposes a sensorless direct field oriented strategy based on the full order Extended Kalman Filter Observer.

The Extended Kalman Filter (EKF) is applied to nonlinear, time-varying stochastic systems, this observer is a unique observer which offers best possible filtering of the noise in measurement and of the system if the noise covariances are known. The advantage of EKF is that they can combine parameter and state estimation. The algorithm is based on a mathematical model representing the machine dynamics taking into account plant and measurement noise. The EKF has the advantages of considering modeling errors and inaccuracy as well as measurement errors in addition to accurate speed estimation over a wide speed range [12]. This paper is organized as follows:

- Section 2 dynamic model of DFIM is reported;
- principle of field-oriented controller is given in Section 3.
- The proposed solution is presented in Section 4.
- In Section 5, results of simulation tests are reported.
- Finally, Section 6 draws conclusions.

2 Doubly Fed Induction Motor model

The chain of energy conversion adopted for the power supply of the DFIM consists of two converters, one on the stator and the other one on the rotor. A filter is inserted between the two converters, as shown in Fig. 1.

The structure of DFIM is very complex. Therefore, in order to develop a model, it is necessary to consider the following simplifying assumptions: the machine is

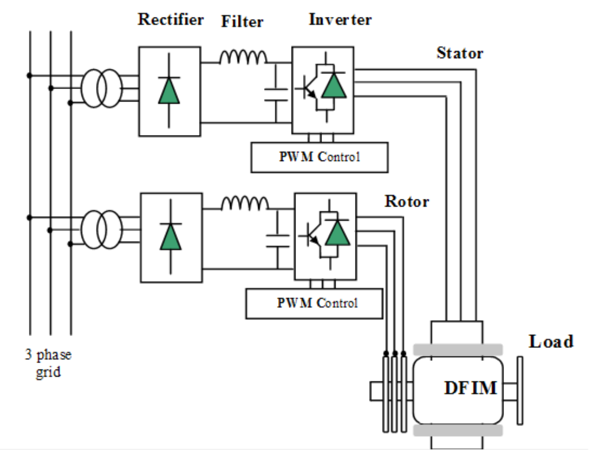

Fig. 1 General scheme of DFIM drive installation

symmetrical with constant air gap; the magnetic circuit is not saturated and it is perfectly laminated, with the result that the iron losses and hysteresis are negligible and only the windings are driven by currents; the m.m.f created in one phase of stator and rotor are sinusoidal distributions along the gap [13].

By this means, a dynamic model of the DFIM in stationary reference frame can be expressed by:

$$\begin{cases} \frac{d}{dt} i_{sd} = -\lambda\, i_{sd} + \omega_s i_{sq} + \frac{K}{T_r}\phi_{rd} + \omega.K\phi_{rq} + \frac{1}{\sigma\, L_s} v_{sd} - K\, v_{rd} \\ \frac{d}{dt} i_{sq} = -\omega_s i_{sq} - \lambda\, i_{sq} - \omega.K\phi_{rd} + \frac{K}{T_r}\phi_{rq} + \frac{1}{\sigma\, L_s} v_{sq} - K\, v_{rq} \\ \frac{d}{dt}\phi_{rd} = \frac{L_m}{T_r} i_{sd} - \frac{1}{T_r}\phi_{rd} + \omega.\phi_{qr} + v_{rd} \\ \frac{d}{dt}\phi_{rq} = \frac{L_m}{T_r} i_{sq} - \omega.\phi_{rd} - \frac{1}{T_r}\phi_{rq} + v_{rq} \\ \frac{d}{dt}\omega = \frac{3}{2J} p^2 \frac{L_m}{L_r}\left(\phi_{rd} i_{sq} - \phi_{rq} i_{sd}\right) - \frac{F}{J}\omega - \frac{C_r}{J} \end{cases} \tag{1}$$

with:

$$T_r = \frac{L_r}{R_r};\; T_s = \frac{L_s}{R_s};\; \lambda = \frac{1}{\sigma.T_r};\; K = \frac{L_m}{\sigma L_{s.} L_r};$$

$$\sigma = 1 - \frac{L_m^2}{L_s L_r};\; \omega = p.\Omega\ .$$

The electromagnetic torque is expressed by:

$$T_{em} = \frac{3}{2}\frac{p\, L_m}{L_r}\left(\phi_{rd}.i_{sq} - \phi_{rq}.i_{sd}\right). \tag{2}$$

3 Vector control by rotor flux orientation

The main objective of the vector control of DFIM is as in DC machines, to independently control the torque and the flux; this is done by using a d-q rotating reference frame synchronously with the rotor flux space vector. The d-axis is then aligned with the rotor flux space vector [14]. Under this condition we get:

$$\phi_{rq} = 0,\; \phi_r = \phi_{rd}. \tag{3}$$

So, we can write:

$$T_{em} = \frac{3}{2} \times \frac{p\, L_m}{L_r}\left(\phi_{rd} \times i_{sq}\right). \tag{4}$$

For the Direct Rotor Flux Orientation (DFOC) of DFIM, accurate knowledge of the magnitude and position of the rotor flux vector is necessary. In a DFIM motor mode, as stator and rotor currents are measurable, the rotor flux can be estimated (calculated). The flux estimator can be obtained by the Eq. (5) [15]:

$$\phi_r = \sqrt{\phi_{r\alpha}{}^2 + \phi_{r\beta}{}^2} \text{ and } \theta_S = \tan^{-1}\left(\frac{\phi_{r\beta}}{\phi_{r\alpha}}\right). \tag{5}$$

3.1 The speed control of the DFIM by an adaptive Fuzzy-PI controller

In order to achieve good performance of sensorless vector control, we propose a robust adaptive Fuzzy-PI speed controller.

In what follows, we show the synthesis and description of the adaptation of the PI controller by a fuzzy system method:

- The fuzzy inference mechanism adjusts the PI parameters and generates new parameters during the process control. It enlarges the operating area of the linear controller (PI) so that it also works with a non-linear system [16, 17].
- The input of the fuzzy adapter are:
  - the error (e) and
  - the derivative of error (Δe).
- The outputs are:
  - the normalized value of the proportional action (k'_p) and
  - the normalized value of the integral action (k'_i).

The normalization PI parameters are given by Eqs. (6), (7) [18]:

$$k'_p = \left(k_p - k_{p\min}\right) / \left(k_{p\max} - k_{p\min}\right) \tag{6}$$

$$k'_i = \left(k_i - k_{i\min}\right) / \left(k_{i\max} - k_{i\min}\right). \tag{7}$$

The parameters k'_p and k'_i are determined by a set of fuzzy rules of the form. If e is A_i, and Δe is B_i, then k'_p is C_i, and k'_i is D_i. Where A_i, B_i, C_i and D_i are fuzzy sets on corresponding supporting sets. The associated fuzzy sets involved in the fuzzy control rules are defined as follows:

- ZE Zero
- PB Positive Big
- PM Positive Medium
- PS Positive Small
- S Small
- NB Negative Big
- NM Negative Medium
- NS Negative Small
- B Big.

The membership functions for the fuzzy sets corresponding to the error e, Δe and the adjusted proportional and integral terms (k'_p and k'_i) are defined in Fig. 2 and Fig. 3.

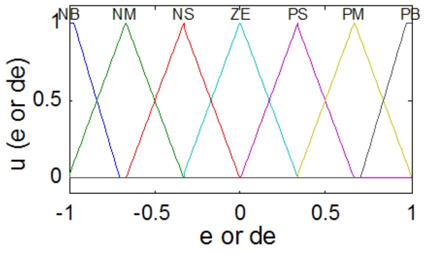

Fig. 2 Membership functions e and Δe.

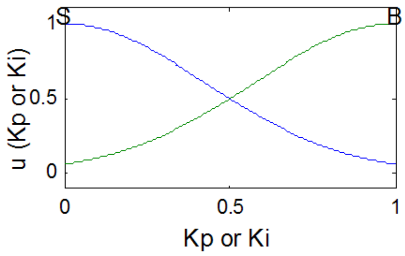

Fig. 3 Membership functions k'_p and k'_i

By using the membership functions shown in Fig. 3, we satisfy the Eq. (8).

$$\sum_1^m \upsilon_i = 1 \tag{8}$$

The fuzzy outputs k'_p and k'_i can be calculated by the center of area defuzzification as:

$$\left[k'_p, k'_i\right] = \frac{\sum_{i=1}^{3} w_i c_i}{\sum_{i=1}^{3} w_i} = \frac{\begin{bmatrix} c_1 & \dots & c_2 \end{bmatrix} \begin{bmatrix} w_1 \\ \vdots \\ w_2 \end{bmatrix}}{\sum_{i=1}^{2} w_i} = \upsilon^T W. \tag{9}$$

Where $C = \begin{bmatrix} c_1 & \dots & c_2 \end{bmatrix}$ is the vector containing the output fuzzy centers of the membership functions, $W = \begin{bmatrix} w_1 & \dots & w_2 \end{bmatrix} \Big/ \sum_{i=1}^{2} w_i$ is the firing strength vector and υ_i represents the membership value of the output k'_p or k'_i to output fuzzy set i.

Once the values of k'_p and k'_i are obtained, the new parameters of PI controller is calculated by Eqs. (10), (11) [17]:

$$k_p = \left(k_{p\max} - k_{p\min}\right).k'_p + k_{p\min} \tag{10}$$

$$k_i = \left(k_{i\max} - k_{i\min}\right).k'_i + k_{i\min}. \tag{11}$$

4 Kalman filter observer

The Kalman filter is a state observer that relies on a number of assumptions including the presence of noise. The basic principle of the Kalman filter is the minimization, variance of state-based estimation measurement error.

The Kalman filter can be expressed by Eqs. (12), (13) [19]:

$$\frac{d}{dt}x = Ax + Bu + U(t).w(t) \text{ (Systemequation)} \quad (12)$$

$$y = Cx + v(t) \text{ (Measurement equation)} \quad (13)$$

where
$U(t)$ = weight matrix of noise
$v(t)$ = noise matrix of output model (measurement noise)
$w(t)$ = noise matrix of state model (system noise)
$U(t)$, $v(t)$, and $w(t)$ are assumed to be stationary, white Gaussian noise and their expectation values are zero.

The covariance matrices (Q) and (R) of this noise are defined as

$$Q = \text{convaiance } (w) = E\{ww'\} \quad (14)$$

where $E\{.\}$ denotes the expected value.

The basic scheme of the Kalman filter is given in the Fig. 4.

$$R = \text{convaiance } (v) = E\{vv'\} \quad (15)$$

The state equations of the Kalman filter can be performed by Eq. (16):

$$\dot{\hat{x}} = (A - KC)\hat{x} + Bu + K\ y. \quad (16)$$

The Kalman filter matrix is based on the covariance of the noise and denoted by K. The measure of quality of the observation is expressed by Eq. (17):

$$L_x = \sum E\left\{[x(k) - (k)]^T [x(k) - \hat{x}(k)]\right\} = \min. \quad (17)$$

The value of K should be such that as to minimize L_x. The result of K is a recursive algorithm for the discrete time case. The discrete form of Kalman filter may be written by Eqs. (18)-(22) [20]:

1. System state estimation

$$x(k+1) = x(k) + K(k)\big(y(k) - \hat{y}(k)\big) \quad (18)$$

2. Renew of the error covariance matrix

$$P(k+1) = P(k) - K(k)h^T(k+1)P(k) \quad (19)$$

3. Calculation of Kalman filter gain matrix

$$K(k+1) = P^*(k+1)h^T(k+1) \left[h(k+1)P^*(k+1)h^T(k+1) + R\right]^{-1} \quad (20)$$

4. Prediction of state matrix

$$f(k+1) = \frac{\partial}{\partial x}(A_d x + B_d v)\Big|_{x=\hat{x}(k+1)} \quad (21)$$

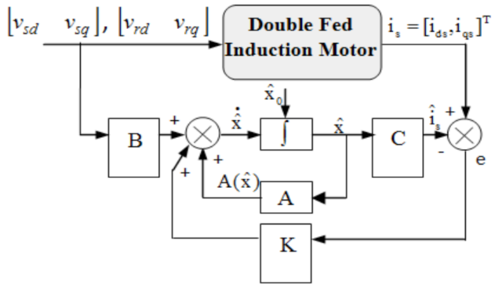

Fig. 4 The basic configuration of the Kalman filter observer

5. Estimation of error covariance matrix

$$P^*(k+1) = f(k+1)\hat{P}(k)f^T(k+1) + Q. \quad (22)$$

Discretization of Eq. (12) and Eq. (13) yields

$$x(k+1) = A_d(k)x(k) + B_d(k)u(k) \quad (23)$$

$$y(k) = C_d(k)x(k) \quad (24)$$

where $K(k)$ is the feedback matrix of the Kalman filter.

$K(k)$ gains matrix calculates how the state vector of the Kalman filter is updated when the output of the model is compared with the actual output of the system. The EKF is a recursive optimum stochastic state estimator which can be used for the joint state and parameter estimation of a non-linear dynamic system in real time by using noisy monitored signals that are disturbed by random noise.

An extended DFIM model is obtained and the rotor speed is considered as an extended state. The discrete DFIM model defined in Eq. (23) and Eq. (24) can be implemented in the Extended Kalman Filter algorithm. The block diagram of the EKF estimator is shown in Fig. 5.

The input and output matrices of the discrete system are denoted by A_d, B_d, and C_d, while the state and the output of the discrete system are denoted by $x(k)$ and $y(k)$.

The discrete model of the DFIM can be given by Eq. (25) [19, 20]:

$$\begin{aligned} x(k+1) &= f\big(x(k), u(k)\big) + w(k) = A_d x(k) + B_d u(k) + w(k) \\ y(k) &= h\big(x(k)\big) + V(k) = C_d x(k) + V(k). \end{aligned} \quad (25)$$

Where $w(k)$ is the measurement noise and $V(k)$ is the process noise.

The state vector is chosen to be

$$\begin{aligned} A_d &= e^{AT_s} \approx I - AT_s \\ B_d &= \int_0^T e^{A_\tau} B d\tau \approx BT_s. \\ C_d &= C \end{aligned} \quad (26)$$

4.1 Application of Kalman filter extended to DFIM

Now, we will proceed to the equation of states of the model of the machine that will be used to design our observer, it is necessary to take a reference axis related to the stator, so:

$$X = \begin{bmatrix} i_{s\alpha} & i_{s\beta} & \phi_{r\alpha} & \phi_{r\beta} \end{bmatrix}^T;$$

$$U = \begin{bmatrix} v_{s\alpha} & v_{s\beta} & v_{r\alpha} & v_{r\beta} \end{bmatrix}^T;$$

$$B = \begin{bmatrix} \frac{1}{\sigma L_s} & 0 & K & 0 \\ 0 & \frac{1}{\sigma L_s} & 0 & K \\ 0 & 0 & 1 & 0 \\ 0 & 0 & 0 & 1 \end{bmatrix}.$$

The state equations can be written by Eq. (27):

$$\begin{cases} \dot{i}_{s\alpha} = -\lambda\, i_{s\alpha} + \omega_s i_{s\beta} + \frac{K}{T_r}\phi_{r\alpha} + \omega.K\phi_{r\beta} + \frac{1}{\sigma L_s} v_{s\alpha} + K\, v_{s\alpha} \\ \dot{i}_{s\beta} = -\omega_s i_{s\beta} - \lambda\, i_{s\beta} - \omega.K\phi_{r\alpha} + \frac{K}{T_r}\phi_{r\beta} + \frac{1}{\sigma L_s} v_{s\beta} + K\, v_{s\beta} \\ \dot{\phi}_{r\alpha} = \frac{L_m}{T_r} i_{s\alpha} - \frac{1}{T_r}\phi_{r\alpha} + \omega.\phi_{r\beta} + v_{r\alpha} \\ \dot{\phi}_{r\beta} = \frac{L_m}{T_r} i_{s\beta} - \omega.\phi_{r\alpha} - \frac{1}{T_r}\phi_{r\beta} + v_{r\beta} \end{cases} \tag{27}$$

with

$$T_r = \frac{L_r}{R_r};\; T_s = \frac{L_s}{R_s};\; \lambda = \frac{1}{\sigma.T_r};\; K = \frac{L_m}{\sigma L_s.L_r}.$$

The extended model of the machine in the repository linked to the stator is written:

$$f = \begin{bmatrix} -\lambda.x_1 + \omega_s.x_2 + \frac{K}{T_r}x_3 + K.\omega.x_4 + \frac{1}{\sigma L_s}v_{s\alpha} + K.v_{s\alpha} \\ -\lambda.x_2 + \omega_s.x_2 - K.\omega.x_3 + \frac{K}{T_r}.x_4 + \frac{1}{\sigma L_s}v_{s\beta} + K.v_{s\beta} \\ \frac{L_m}{T_r}x_1 - \frac{1}{T_r}x_3 + \omega.x_4 + v_{r\alpha} \\ \frac{L_m}{T_r}x_2 - \omega.x_3 - \frac{1}{T_r}x_4 + v_{r\beta} \\ 0 \end{bmatrix}. \tag{28}$$

The stator voltages and states are:

$$U = \begin{bmatrix} v_{s\alpha} & v_{s\beta} & v_{r\alpha} & v_{r\beta} \end{bmatrix}^T$$

$$X = \begin{bmatrix} x_1 & x_2 & x_3 & x_4 & x_5 \end{bmatrix}^T = \begin{bmatrix} i_{s\alpha} & i_{s\beta} & \phi_{r\alpha} & \phi_{r\beta} & \omega_r \end{bmatrix}^T.$$

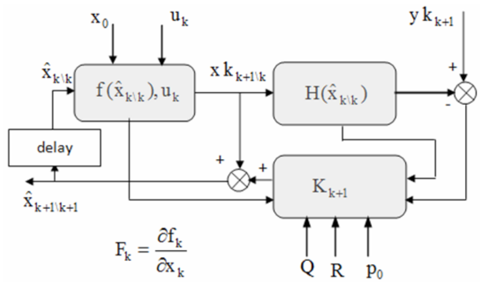

Fig. 5 EKF bloc diagram

The Jacobian matrix (F) is deduced by Eq. (29):

$$F = \begin{bmatrix} 1 - t_e.\lambda & t_e.\omega_s & t_e.\frac{K}{T_r} & t_e K.\omega & t_e.K.\phi_{r\beta} \\ t_e.\omega_s & 1 - t_e.\lambda & -t_e K.\omega & t_e.\frac{K}{T_r} & -t_e.K.\phi_{r\alpha} \\ t_e.\frac{L_m}{T_r} & 0 & 1 - t_e.\frac{1}{T_r} & +t_e.\omega & +t_e.\phi_{r\beta} \\ 0 & t_e.\frac{L_m}{T_r} & -t_e.\omega & 1 - t_e.\frac{1}{T_r} & -t_e.\phi_{r\alpha} \\ 0 & 0 & 0 & 0 & 1 \end{bmatrix}. \tag{29}$$

The important and difficult part in the design of the full order EKF is choosing the proper values for the covariance matrices (Q) and (R). The change of values of covariance matrices affects both the dynamic and steady-state.

In order to have a good performance, to insure better stability, convergence time and considerable rapidity of the EKF, the chosen values for the covariance matrices (Q), (R) and (P) can be initialized and adjusted as

$$P = diag\begin{bmatrix} 0.1 & 0.1 & 1e^{-3} & 1e^{-3} & 60 \end{bmatrix}$$

$$Q = diag\begin{bmatrix} 0.01 & 0.01 & 1e^{-3} & 1e^{-3} & 1e^{-2} \end{bmatrix}$$

$$R = \begin{bmatrix} 2.5 & 2.5 \end{bmatrix}.$$

5 Simulation result and discussion

In order to evaluate the performance of the full order Extended Kalman Filter estimation algorithm and therefore the overall drive system performance, we subjected our system to various simulation tests for direct oriented rotor flux control (Fig. 6).

The main parameters of this simulation are summarized as follows:

- sampling frequency 1.8 kHz;
- the DC voltage U_{DC} = 500 V.

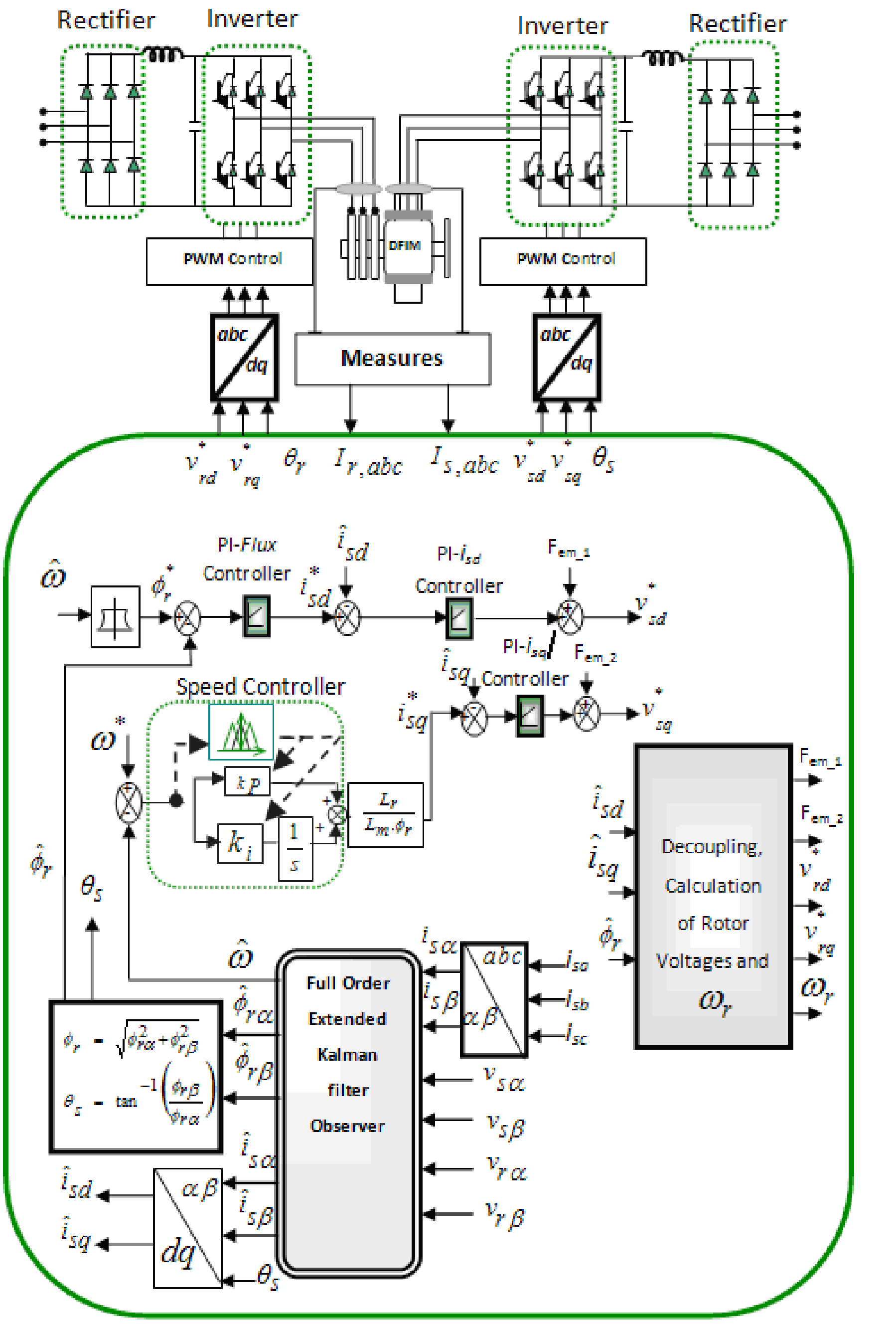

Fig. 6 Block diagram of sensorless direct vector control of DFIM using a full order EKF Observer

This scheme (Fig. 6) consists of a DFIM powered by two PWM voltage inverters, a Direct Field Oriented Control block in which there is an adaptive Fuzzy-PI speed controller, PI type current and flux controllers as well, a transformation block of three-phase quantities to two-phase magnitudes, an observer on the Extended Kalman Filter.

The first test (Fig. 7) concerns a no-load starting of the motor with a reference speed ω_{ref} = 250 rad/s and a nominal load disturbance torque (10 N.m) is suddenly applied between 1 sec and 2 sec, followed by a consign inversion (−250 rad/s) at 2.5 s, this test has for object the study of controller behaviors in pursuit and in regulation.

It can be seen that the estimate of the rotational speed is almost perfect (Fig. 7 (a)). The estimated speed follows perfectly the real speed with a static error equal to zero (Fig. 5 (b)). We also notice that there is good sensitivity to load disturbances is observed, with a relatively low rejection time because of the use of a strong and robust control loop by the adaptive Fuzzy-PI controller.

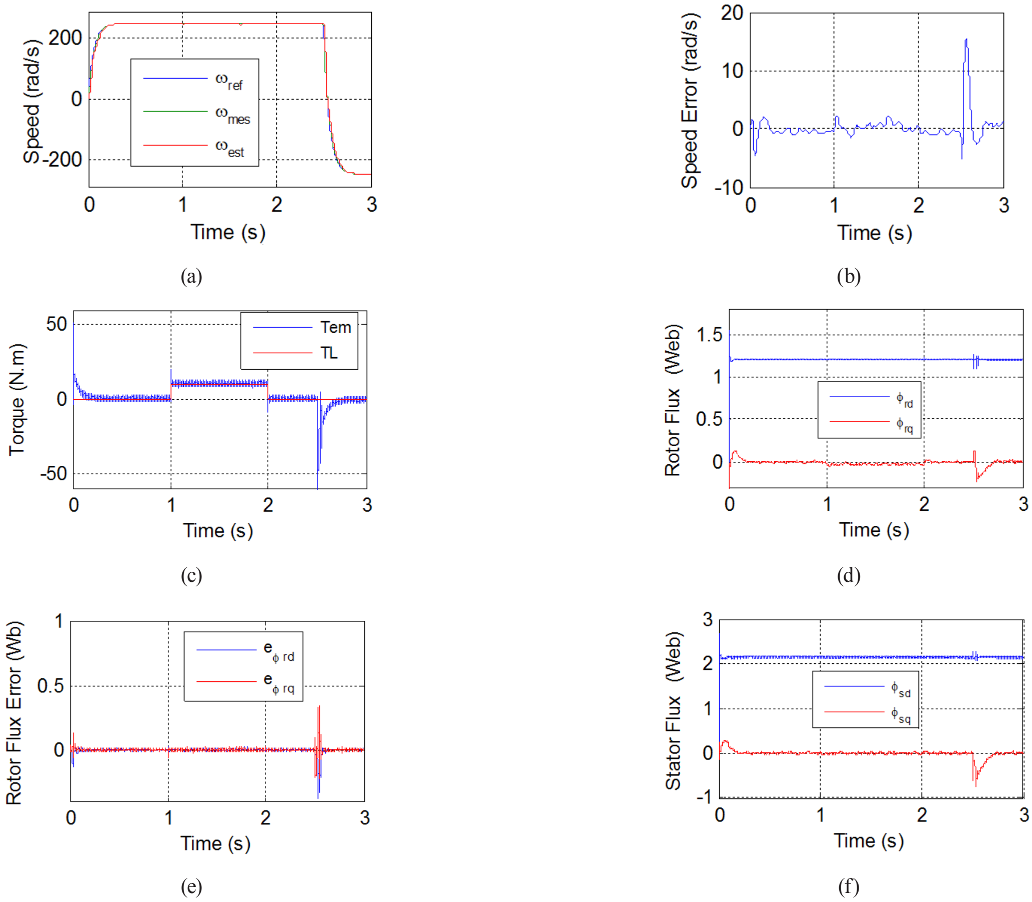

Fig. 7 Simulation waveforms of proposed sensorless control drives: Reference, Mesure and Estimated Rotor speed, Speed Error, Stator Flux, Rotor Flux, Rotor Flux Error, Electromagnetic torque waveform.

Fig. 7 (c) shows the electromagnetic torque waveform in the case of sensorless DFIM with adaptive Fuzzy-PI speed based on Direct Field Oriented Control.

We clearly see an excellent orientation of the rotor flux on the direct axis (Fig. 7 (d)), during the changes of the setpoints, and in particular during the inversion of rotation, the change of direction of the torque does not degrade the orientation of the fluxes. We also note a perfect continuation of the components of the rotor flux estimated at their corresponding real components (Fig. 7 (e)).

5.1 The rotor resistance variation test

In order to study the influence of parametric variations on the behavior of the EKF-based speed sensorless vector control, we introduced a variation of +50 % of R_r in the first test, we obtained the results as shown in Fig. 8 whose membership functions of adaptive Fuzzy-PI are detailed in Tables 1 and 2.

According to the result of Fig. 8, we note that the increase in resistance did not affect the accuracy of

Table 1 Fuzzy rules base for computing k'_p

Δe \ e	NB	NM	NS	ZE	PS	PM	PB
NB	B	B	B	B	B	B	B
NM	S	B	B	B	B	B	S
NS	S	S	B	B	B	S	S
ZE	S	S	S	B	S	S	S
PS	S	S	B	B	B	S	S
PM	S	B	B	B	B	B	S
PB	B	B	B	B	B	B	B

Table 2 Fuzzy rules base for computing k'_i

Δe \ e	NB	NM	NS	ZE	PS	PM	PB
NB	B	B	B	B	B	B	B
NM	B	S	S	S	S	S	B
NS	B	B	S	S	S	B	B
ZE	B	B	B	S	B	B	B
PS	B	B	S	S	S	B	B
PM	B	S	S	S	S	S	B
PB	B	B	B	B	B	B	B

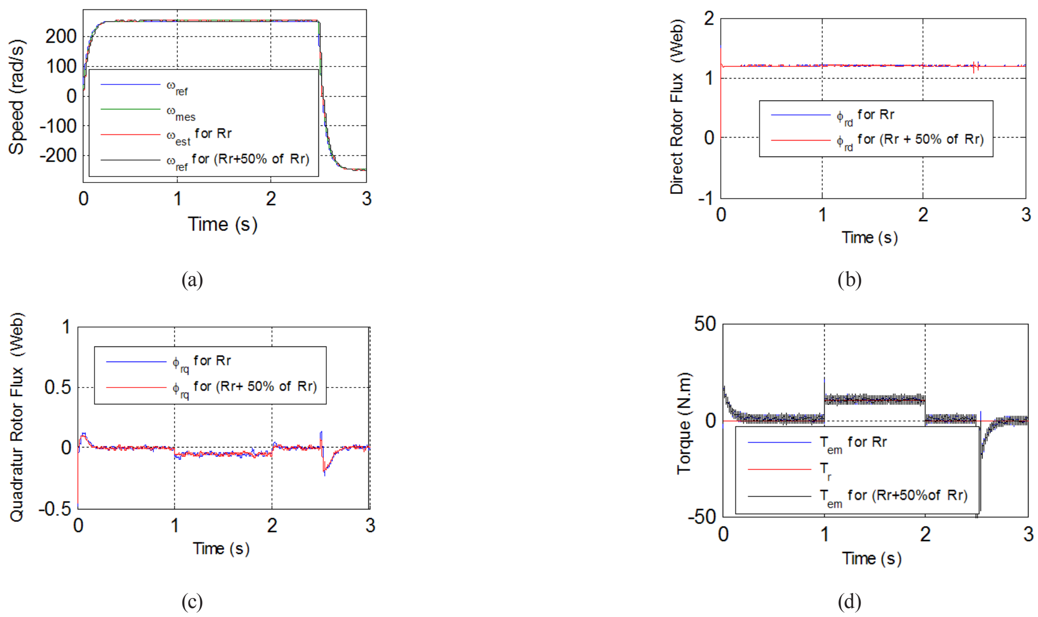

Fig. 8 Simulation results of proposed sensorless control drives under a load change and with rotor resistance increased sharply by 50 % from rated value

the observer and the estimation of the rotational speed, we clearly see that the estimated speed perfectly follows its reference. An increase of the rotor resistance gives best performances.

The results of the speed control have shown that the control with adaptive Fuzzy-PI controller ensures good performance even in the presence of parametric variations and external disturbances (load disturbance torque).

As we see in this result, the increase in resistance did not affect the accuracy and orientation of the rotor flux, which proves the robustness of the proposed controller. According to these results, we can say and in general, we obtained the same performance as the previous test with the nominal rotor resistance.

5.2 The stator resistance variation test

For a nominal value of R_r, the stator resistance R_s is increased by +50 % of its nominal value, we obtained the results as shown in Fig. 9. The obtained results (Fig. 9) demonstrates that even if the stator resistance changes,

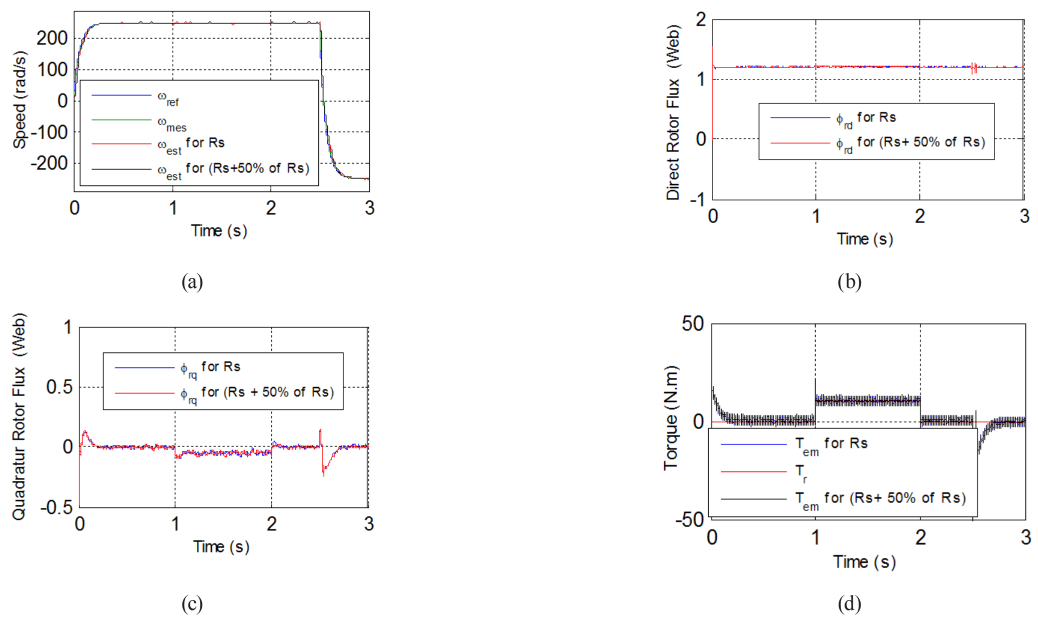

Fig. 9 Simulation results of proposed sensorless control drives under a load change and with stator resistance increased sharply by 50 % from rated value

the proposed full order Extended Kalman Filter Observer gives a good estimate of the speed. This result shows also that using adaptive Fuzzy-PI controller performs a better control in terms of robustness

6 Conclusion

In this paper, adaptive Fuzzy-PI controller was employed to solve different drawbacks of the conventional PI controllers and to obtain the better performance from the DFIM motor mode in a speed control also make it insensitive to parameter variations, and disturbances. sensorless speed operation increases reliability, reduces the complexity and the cost of the system, for all these reasons full order Extended Kalman Filter Observer is developed.

The simulation results prove that the proposed method give high the robustness quality. The optimal sensorless vector control is then obtained and the torque/current ratio is thus maintained at the maximum value corresponding to a given load torque and also in the case of variation of the parameters.

References

[1] Karthikeyan, A., Nagamani, C., Chaudhury, A. B. R. "An implicit sensorless position/speed estimator for the speed control of a Doubly Fed Induction motor", In: Innovative Smart Grid Technologies (ISGT) – India, ISGT2011-India, Kollam, Kerala, India, 2011, pp. 120–125. https://doi.org/10.1109/ISET-India.2011.6145367

[2] El Khil, S. K., Slama-Belkhodja, I., Pietrzak-David, M., De Fornel, B. "Design of rotor and stator converters for a Double Fed Induction Machine", In: 2006 IEEE International Symposium on Industrial Electronics, Montreal, Québec, Canada, 2006, pp. 2485–2491. https://doi.org/10.1109/ISIE.2006.295963

[3] El Khil, S. K., Slama-Belkhodja, I., Pietrzak-David, M., de Fornel, B. "Sensorless Field Oriented Control of Doubly Fed Induction Speed Drive", In: EUROCON 2007 – The International Conference on "Computer as a Tool", Warsaw, Poland, 2007, pp. 1888–1895. https://doi.org/10.1109/EURCON.2007.4400558

[4] Payam, A. F., Hashemnia, N., Kashiha A. "Robust Speed Sensorless Control of Doubly-fed Induction Machine Based on Input-output Feedback Linearization Control Using a Sliding-mode Observer", World Applied Sciences Journal, 10(11), pp. 1392–1400, 2010. [online] Available at : https://www.idosi.org/wasj/wasj10(11)10/20.pdf [Accessed: 19 April 2019]

[5] Peresada, S., Tilli, A., Tonielli, A. "Indirect stator flux-oriented output feedback control of a doubly fed induction machine", IEEE Transactions on Control Systems Technology, 11(6), pp. 875–888, 2003. https://doi.org/10.1109/TCST.2003.819590

[6] El Ouanjli, N., Derouich, A., El Ghzizal, A., Chebabhi, A., Taoussi, M. "A comparative study between FOC and DTC controls of the Doubly Fed Induction Motor (DFIM)", In: 3rd International Conference on Electrical and Information Technologies (ICEIT'2017), Rabat, Morocco, 2017, pp. 1–6. https://doi.org/10.1109/EITech.2017.8255302

[7] Ben Attous, D., Bekakra, Y. "Speed Control of a Doubly Fed Induction Motor using Fuzzy Logic Techniques", International Journal on Electrical Engineering and Informatics, 2(3), pp. 179–191, 2010. https://doi.org/10.15676/ijeei.2010.2.3.2

[8] Soltani, J., Payam, A. F., Abbasian, M. A. "A Speed Sensorless Sliding-Mode Controller for Doubly-Fed Induction Machine Drives with Adaptive Backstepping Observer", In: 2006 IEEE International Conference on Industrial Technology, Mumbai, India, 2006, pp. 2725–2730. https://doi.org/10.1109/ICIT.2006.372652

[9] Cherifi, D., Miloud, Y. "Speed Sensorless Control of a Doubly Fed Induction Motor Drives using MRAS Estimator", International Journal of Electrical Components and Energy Conversion, 4(1), pp. 1–12, 2018. https://doi.org/10.11648/j.ijecec.20180401.11

[10] Zerikat, M., Mechernene A., Chekroun, S. "High-performance sensorless vector control of induction motor drives using artificial intelligent technique", European Transactions on Electrical Power, 21(1), pp. 787–800, 2011. https://doi.org/10.1002/etep.477

[11] Iacchetti, M. F., Carmeli, M. S., Dezza, F. C., Perini, R. "A speed sensorless control based on a MRAS applied to a double fed induction machine drive", Electrical Engineering, 91(6), pp. 337–345, 2010. https://doi.org/10.1007/s00202-009-0144-8

[12] Alonge, F., D'Ippolito, F., Sferlazza, A. "Sensorless Control of Induction-Motor Drive Based on Robust Kalman Filter and Adaptive Speed Estimation", IEEE Transactions on Industrial Electronics, 61(3), pp. 1444–1453, 2014. https://doi.org/10.1109/TIE.2013.2257142

[13] Lekhchine, S., Bahi, T., Aadlia, I., Layate, Z., Bouzeria, H. "Speed Control of Doubly Fed Induction Motor", Energy Procedia, 74, pp. 575–586, 2015. https://doi.org/10.1016/j.egypro.2015.07.758

[14] Cifci, A., Uyaroglu, Y., Birbas, S. "Direct Field Oriented Controller Applied to Observe Its Advantages over Scalar Control", Electronics and Electrical Engineering, 119(3), pp. 15–18, 2012. https://doi.org/10.5755/j01.eee.119.3.1355

[15] Mohanty, K. B. "Sensorless Sliding Mode Control of Induction Motor Drives", In: TENCON 2008 – 2008 IEEE region 10 Conference, Hyderabad, India, 2008, pp. 1–6. https://doi.org/10.1109/TENCON.2008.4766709

[16] Bousserhane, I. K, Hazzab, A., Rahli, M., Kamli, M., Mazari, B. "Adaptive PI Controller using Fuzzy System Optimized by Genetic Algorithm for Induction Motor Control", In: 2006 IEEE International Power Electronics Congress, Puebla, Mexico, 2006, pp. 1–8. https://doi.org/10.1109/CIEP.2006.312162

[17] Laroussi, K., Zelmat, M., Rouff, M. "Implementation of a Fuzzy Logic System to Tune a PI Controller Applied to an Induction Motor", Advances in Electrical and Computer Engineering, 9(3), pp. 107–113, 2009. https://doi.org/10.4316/aece.2009.03019

[18] Bedoud, K., Ali-rachedi, M., Bahi, T., Lakel, R. "Adaptive Fuzzy Gain Scheduling of PI Controller for Control of the Wind Energy Conversion Systems", Energy Procedia, 74, pp. 211–225, 2015. https://doi.org/10.1016/j.egypro.2015.07.580

[19] Tety, P., Konaté, A., Asseu, O., Soro, E., Yoboué, P., Kouadjo, A. R. "A Robust Extended Kalman Filter for Speed-Sensorless Control of a Linearized and Decoupled PMSM Drive", Engineering, 7(10), pp. 691–699, 2015. https://doi.org/10.4236/eng.2015.710060

[20] Lešić, V., Vašak, M., Stojičić, G., Perić, N., Joksimović, G., Wolbank, T. M. "State and Parameter Estimation for Field-oriented Control of Induction Machine Based on Unscented Kalman Filter", In: IEEE International Symposium on Power Electronics, Electrical Drives, Automation and Motion, Sorrento, Italy, 2012, pp. 409–414. https://doi.org/10.1109/SPEEDAM.2012.6264421

Appendix

DFIM motor parameters

Item	Symbol	Data
DFIM Mechanical Power	P_W	1.5 Kw
Nominal speed	ω	1450 rpm
Pole pairs number	P	2
Stator resistance	R_s	1.68 W
Rotor resistance	R_r	1.75 W
Stator self inductance	L_s	295 mH
Rotor self inductance	L_r	104 mH
Mutual inductance	L_m	165 mH
Moment of inertia	J	0.01 kg.m^2
Friction coefficient	F	0.0027 kg.m^2/s
Nominal Frequency	f	50 Hz

Nomenclature of the parameters DFIM model

v_{sd}, v_{sq}	Stator and rotor voltages d-q axis components
v_{rd}, v_{rq}	Rotor voltages d-q axis components
i_{sd}, i_{sq}, i_{rd}, i_{rq}	Stator and rotor currents d-q axis components
ω_s, ω_r	stator and rotor pulsation respectively
R_s, R_r	Stator- Rotor resistance
L_s, L_r	Stator- and Rotor inductance respectively
L_m	Mutual inductance
ω	Mechanical speed
T_{em}	Electromagnetic torque
T_L	Load torque
J	Total inertia
p	Number of pole pairs
F	Friction coefficient